

# The Effect of Nanosecond, High-Voltage Electric Pulses on the Shape and Permeability of Polymersome GUVs

Tina Batista Napotnik<sup>1</sup> · Gianluca Bello<sup>2</sup> · Eva-Kathrin Sinner<sup>2</sup> · Damijan Miklavčič<sup>1</sup>

Received: 10 March 2017 / Accepted: 6 July 2017 / Published online: 22 July 2017  
© Springer Science+Business Media, LLC 2017

**Abstract** Polymersomes, vesicles composed of block copolymers, are promising candidates as membrane alternatives and functional containers, e.g., as potential carriers for functional molecules because of their stability and tunable membrane properties. In the scope of possible use for membrane protein delivery to cells by electrofusion, we investigated the cytotoxicity of such polymersomes as well as the effects of nanosecond electric pulses with variable repetition rate on the shape and permeability of polymersomes in buffers with different conductivities. The polymersomes did not show cytotoxic effects to CHO and B16-F1 cells in vitro in concentrations up to 250 µg/mL (for 48 h) or 1.35 mg/mL (for 60 min), which renders them suitable for interacting with living cells. We observed a significant effect of the pulse repetition rate on electrodeformation of the polymersomes. The electrodeformation was most pronounced in low conductivity buffer, which is favorable for performing electrofusion with cells. However, despite more pronounced deformation at higher pulse repetition rate, the electroporation performance of polymersomes was unaffected and remained in similar ranges both at 10 Hz and 10 kHz. This phenomenon is possibly due to the higher stability and rigidity of polymer vesicles, compared to liposomes, and can serve as an advantage (or disadvantage) depending on the aim in employing

polymersomes such as stable membrane alternative architectures or drug vehicles.

**Keywords** Electroporation · Polymersomes · Electrodeformation · Nanosecond electric pulses · Membrane alternatives

## Introduction

The cell membrane is a bilayered semi-permeable lipid barrier that shapes and protects the cell, shielding the inner cell components and organelles from the outer environment (Singer and Nicolson 1972). It is the structure where complex and essential functions involved in the cell's homeostasis, signaling, and communication take place (Lodish et al. 2000). Across the cell membrane, passive diffusion and protein channel-regulated exchange of ions and solutes generate a resting transmembrane potential (rTMV) (Alberts et al. 2002). Electrically excitable cells, such as neurons, regulate their rTMV in order to propagate along the membrane an electric signal (Alberts et al. 2002). Self-assemblies of lipids in the form of giant unilamellar vesicles (GUVs, diameter > 1 µm) are used to determine the electromechanical boundaries of the cell membrane subjected to an external electric field (EF) (Dimova et al. 2007, 2009) in order to study these electromechanical phenomena. The effects of these forces result in reversible shape remodeling, electroporation (also termed electroporation) as well as electrofusion of cells or vesicles (Dimova et al. 2009; Knorr et al. 2010; Jordan et al. 2013; Rems et al. 2013). The EF may also induce irreversible rupture of the structure resulting in cell death or vesicle bursting (Gabriel and Teissié 1995; Dimova et al. 2009). Lately, the interest for polymers that form bilayers

✉ Damijan Miklavčič  
Damijan.Miklavcic@fe.uni-lj.si

<sup>1</sup> Faculty of Electrical Engineering, University of Ljubljana, Tržaška 25, 1000 Ljubljana, Slovenia

<sup>2</sup> Institute of Synthetic Bioarchitectures, University of Natural Resources and Life Sciences (BOKU), Muthgasse 11, 1190 Vienna, Austria

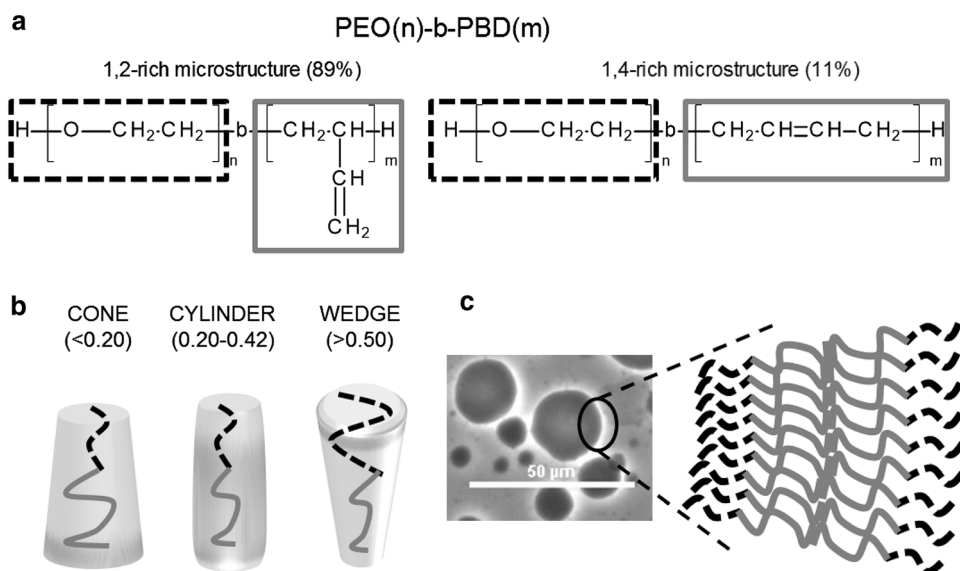
emerged in virtue of their extensively tunable (hydrophobic/hydrophilic content, chains length, charge, biodegradability) and functional (antibody functionalization, bio- and environmental sensing, detectability) properties (Le Meins et al. 2011). In this regard, the electromechanical properties of biocompatible block copolymers have been partially investigated (Aranda-Espinoza et al. 2001) envisaging alternative membrane models with improved mechanical properties, compared to the lipid bilayer. In fact, by precisely controlling the number and type of the polymer's components (blocks), they can be used as mimetics of natural membranes resembling the lipid bilayer, with additional capabilities and mechanic properties (Taubert et al. 2004).

In this study we use the amphiphilic, diblock, copolymer poly(ethylene oxide)-*b*-poly(butadiene) (PEO<sub>*n*</sub>-*b*-PBD<sub>*m*</sub> or OB<sub>*n-m*</sub>) (Fig. 1a) built up from 13 hydrophilic PEO blocks and 22 hydrophobic PBD blocks (OB<sub>13-22</sub>). The PEO blocks constitute the hydrophilic head group, while the PBD blocks build up the hydrophobic moiety of the whole amphiphilic OB molecule. Amphiphiles, in aqueous buffers, organize themselves into macro-structures according to their molecular shape factor (cone, wedge, or cylinder), which is determined by the hydrophilic volume fraction value ( $f_{\text{hydrophilic}}$ ) (Israelachvili 2011), as shown in Fig. 1b. The value of  $f_{\text{hydrophilic}}$  is the ratio between the molecular volume of the hydrophilic portion and the total molecular volume. The conical shape factor is the molecular packing architecture of those lipids that naturally form membranes and bilayered vesicles, and present  $f_{\text{hydrophilic}}$  values of 0.20–0.42 (Discher et al. 2002; Ahmed and Discher 2004). OB<sub>13-22</sub> has a  $f_{\text{hydrophilic}}$  of 0.28 value that allows for the formation of vesicles, or polymersomes (Fig. 1c).

Lipid bilayers, whether they constitute the cell membrane or the membrane of a vesicle, when subjected to an EF, behave as capacitors by accumulating charges on both facets. Consequently, an electric potential difference arises across the bilayer, known as induced transmembrane voltage (iTMV), which superimposes onto the physiological rTMV (Kotnik et al. 1998; Kotnik and Miklavcic 2000). The iTMV may exceed a certain threshold and induce mechanical deformations (prolate or oblate shapes) of the vesicle by the modification of the membrane tension (Dimova et al. 2007, 2009). The EF parameters (duration, magnitude, pulse number, repetition rate) needed to initiate mechanical deformations are determined by the mechanic properties of the bilayer (membrane tension, thickness, interfacial charges) and the conductivities of the inner and outer buffers. The membrane tension of polymer bilayers is generally greater than lipid bilayers therefore a higher iTMV is necessary to induce rupture of the bilayer, compared to the one of lipid (Aranda-Espinoza et al. 2001). Such greater stability of the polymer bilayer is related to the thickness and molecular weight of the polymer used (Bermudez et al. 2002; Photos et al. 2007).

Lipid vesicles deformations exposed to AC and DC electric fields in the ms and  $\mu\text{s}$  regime have been well studied and characterized (Teissie and Tsong 1981; Riske and Dimova 2005, 2006; Tekle et al. 2005; Dimova et al. 2007; Sadik et al. 2011; Salipante and Vlahovska 2014; Perrier et al. 2017). Deformations in AC field depend on differences between inner ( $\lambda_{\text{in}}$ ) and outer ( $\lambda_{\text{out}}$ ) conductivities and the EF frequency: when  $\lambda_{\text{in}} > \lambda_{\text{out}}$  liposomes shift from prolate to spherical shape with increasing frequency, whereas when  $\lambda_{\text{in}} < \lambda_{\text{out}}$  liposomes shift from prolate to spherical shape with an intermediate oblate shape

**Fig. 1** **a** Diblock copolymer PEO<sub>*n*</sub>-*b*-PBD<sub>*m*</sub> (OB<sub>*n-m*</sub>) and its microstructures. **b** Possible molecular shapes of amphiphiles and relative  $f_{\text{hydrophilic}}$ , in brackets. **c** Vesicles formed by OB<sub>13-22</sub> in aqueous solution (scale bar: 50  $\mu\text{m}$ ) and details of the bilayer. The bilayer is formed by the PBD hydrophobic part (solid, light gray) and the PEO hydrophilic part (dashed black)



transition (Dimova et al. 2007; Aranda et al. 2008). In DC fields, similar vesicle deformations are expected, comparing inverse duration of the DC pulse and AC field frequency, and they are intensified due to the stronger EF applied (Dimova et al. 2007; Salipante and Vlahovska 2014). Although some studies have investigated the electroporation of polymer vesicles for the encapsulation of molecules (Wang et al. 2012) or for the development of microreactors (Bain et al. 2015), still little information is available for this polymeric system.

This study is focused on the determination of the deformation and electroporation induced by EF in the nanosecond regime on PEO–PBD vesicles in different buffer conditions. These results aim to elucidate the events in exposing the polymersomes to nanosecond electric pulses in the scope of polymersomes as possible drug carriers or vehicles in the delivery of functional membrane proteins into cell membranes via electrofusion. Namely, in order to electrofuse membrane particles (cells, polymersomes) both close contacts and electroporation of membranes have to be achieved (Zimmermann 1982; Usaj et al. 2013). For a successful achievement of polymersomes delivery or fusion with biological cells with the use of electric pulses, both the polymersome elongation and poration may play significant roles. For a possible further use with living cells, polymersomes were also tested for cytotoxicity.

## Materials and Methods

### Electroformation of Polymersomes

Diblock copolymer polybutadiene-polyethylene oxide [PEO]<sub>13</sub>[PBD]<sub>22</sub> (OB<sub>13-22</sub>) was obtained from Polymer Source (Montreal, Canada) and used without further purification (Mw 1800 g/mol, MW PDI 1.17). Chloroform used to dissolve the polymer was of analytical grade and was obtained from Carl Roth International (Karlsruhe, Germany). Ultrapure water at 18 MΩ cm used for the buffers was produced by a Millipore Integral 10 Milli-Q system from Merck (Darmstadt, Germany). Saccharose and NaCl were of analytical grade (> 99% purity) and were obtained from Carl Roth International (Karlsruhe, Germany). Electroformation instrument Vesicle Prep Pro and the indium-tin-oxide (ITO) slides used for the production of the polymersome GUVs were obtained from Nanion Technologies GmbH (Munich, Germany).

Polymersomes GUVs were produced via electroformation, or electroswelling, with modification of the standard procedure (Angelova and Dimitrov 1986) due to the higher content of solutes (especially NaCl and calcein). The inner buffers used were Ac: 0.3 M saccharose, 1 mM calcein,

inner conductivity: 477 μS/cm, and ABc: 0.3 M saccharose, 5 mM NaCl, 1 mM calcein, inner conductivity: 930 μS/cm (see Table 1).

The PEO–PBD polymer dissolved in chloroform at 1.4 mM concentration was spread drop-wise on the surface of the conductive ITO slide for total of 50 μL/slide. The organic solvent was allowed to evaporate quickly under a stream of air and to ensure a complete solvent removal; the slides were kept at least 30 min under vacuum in a desiccation chamber. The dry film on the ITO slides was hydrated with the inner buffer of choice and covered with another ITO slide separated by a 1 mm silicon ring gasket. The slides were inserted into the Nanion instrument and the electroformation was carried out at 3 Vpp, 10 Hz for 2 h for buffers without NaCl. For buffers containing NaCl the parameters were modified as follows: the initial voltage was set at 3 Vpp with an incremental frequency from 0 to 10 Hz over 1 h. Then the voltage was kept at 3 Vpp, 10 Hz for 8 h. Subsequently, the voltage was changed over a time of 2 h with decremented voltage and frequency from 3 to 0 Vpp and 10 to 0 Hz, respectively. For all electroformation methods the temperature was kept at 40 °C and reduced to room temperature at the end of the process.

The polymersomes were collected with a plastic pipette and kept at 4 °C in Eppendorf tubes. An aliquot of Streptomycin/ampicillin was added to a final concentration of 100 μg/mL to prevent bacterial growth. For the buffers containing the fluorescent dye calcein, the vesicles were washed from the excess dye in the outer buffer of choice via repeated centrifugations at 10,000 × *g* for 5 min at 5 °C. This step was repeated until the GUVs suspension was clear and the fluorescence came exclusively from the inner buffer of the polymersomes.

### Production of Small Unilamellar Vesicles (SUVs) for Cytotoxicity

Small unilamellar vesicles (SUVs) were produced by thin film re-hydration of PEO–PBD polymer and subsequent extrusion (Mayer et al. 1986). Briefly, 500 μL of PEO–PBD polymer stock in chloroform used to produce GUVs was dried with the use of a rotary evaporator in a 5 mL round-bottomed glass flask. The dry polymeric film covering the inner surface of the flask was further dried in a vacuum desiccator for 1 h to ensure total solvent removal. A 500 μL of PBS buffer was added to the flask to hydrate the film. Vortexing and subsequent quick bath-sonication of the suspension allowed the total detachment of the polymeric film from the sides of the flask. The suspension of polymer in PBS was then extruded at least 21 times through a 50 nm polycarbonate membrane by the use of a LiposoFast manual extruder (AVESTIN Europe GmbH, Germany). The final SUVs suspension had a concentration

**Table 1** The composition and conductivities of inner and outer buffers used in the study

Location of buffers	Buffers	Composition	Conductivity ( $\mu\text{S}/\text{cm}$ )
Inner	Ac	0.3 M saccharose, 1 mM calcein	477
	ABc	0.3 M saccharose, 5 mM NaCl, 1 mM calcein	930
Outer	A	0.3 M glucose	9
	AB	0.3 M glucose, 5 mM NaCl	550
	B	0.3 M glucose, 10 mM NaCl	1063
	C	0.3 M glucose, 15 mM NaCl	1499

of 1.5 mM (2.7 mg/mL). The size of the vesicles was assessed by three dynamic light scattering measurements on a Zetasizer Nano ZS device (Malvern Instruments Ltd, UK) at 22 °C.

### Poration Buffers

The following inner polymersome buffers were used in experiments: Ac: 0.3 M saccharose, 1 mM calcein, of conductivity 477  $\mu\text{S}/\text{cm}$ , and ABc: 0.3 M saccharose, 5 mM NaCl, 1 mM calcein, of conductivity 930  $\mu\text{S}/\text{cm}$ . The poration (outer) buffers used were A: 0.3 M glucose, of conductivity 9  $\mu\text{S}/\text{cm}$ ; AB: 0.3 M glucose, 5 mM NaCl, of conductivity 550  $\mu\text{S}/\text{cm}$ ; B: 0.3 M glucose, 10 mM NaCl, of conductivity 1063  $\mu\text{S}/\text{cm}$ ; and C: 0.3 M glucose, 15 mM NaCl, of conductivity 1499  $\mu\text{S}/\text{cm}$  (Table 1). The conductivity was measured with a S230 SevenCompact<sup>TM</sup> conductivity meter (Mettler Toledo, Columbus, OH, USA).

### Cytotoxicity of Polymersomes

Cytotoxicity of polymersomes was tested on two cell lines: Chinese hamster ovary (CHO) and B16-F1 murine melanoma cells. Both cell lines were obtained from European Collection of Cell Cultures (CHO-K1, cat. no. 85051005, B16-F1, cat. no. 92101203) and regularly checked for mycoplasma.

Toxicity assay was performed over two-day period using Promega (Madison, USA) CellTiter 96<sup>®</sup> Aqueous One Solution Cell Proliferation MTS Assay (Barltrop et al. 1991), as described by the manufacturer. CHO and B16-F1 cells in culture media were seeded into 96-well plates at the concentration of 2000 cells/well (90  $\mu\text{L}$ ) and allowed 24 h to attach and recover. 10  $\mu\text{L}$  of SUVs in buffer B was added to cells and culture medium in wells to final concentrations of 0, 0.025, 0.25, 2.5, 25, and 250  $\mu\text{g}/\text{mL}$ . SUV stock solution was sterilized prior the incubation for 30 min under germicidal UV lamp in a quartz cuvette. After two days of incubation, 10  $\mu\text{L}$  of MTS reagent was added to each well, incubated for 2 h, and detected for 490 nm light absorption using a microplate reader Tecan Infinite M200 (Tecan Group Ltd, Männedorf, Switzerland). A blank (90  $\mu\text{L}$  of culture medium without cells, 10  $\mu\text{L}$  of

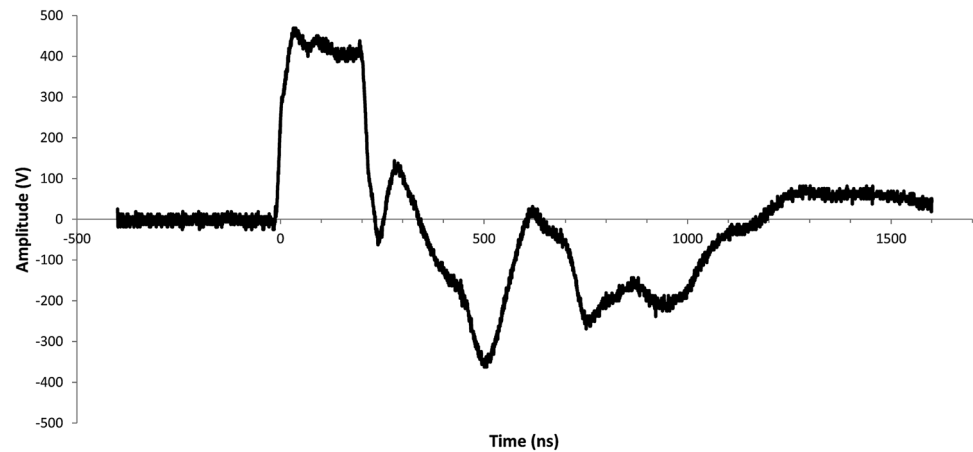
buffer B) was subtracted from absorption results. 1% Triton X-100 was used as positive control (added to cells 30 min prior MTS reagent).

Short-term toxicity was tested using dye-exclusion test with propidium iodide (PI). CHO and B16-F1 cells were grown in HAM and DMEM culture media, respectively (supplemented with fetal bovine serum and antibiotics). They were trypsinized, suspended in culture medium and placed into 96-well plate ( $2 \times 10^6$  cells/mL, 15  $\mu\text{L}/\text{well}$ ). We added 15  $\mu\text{L}/\text{well}$  SUV (final concentration 1.35 mg/mL) or GUV (stock solution from electroformation, unknown concentration). Buffer B alone served as control. Cells and polymersomes (SUV, GUV) or buffer B were incubated for 30 and 60 min. After the incubation time, PI was added into wells at a final concentration of 50  $\mu\text{M}$ , left for 3–5 min to stain exclusively dead cells and observed under an epifluorescence microscope (Leica DFC450 C) with a 40 $\times$  objective, and the appropriate filter setting (EX BP545/30/D565/EM BP610/75). Live and dead cells were counted using JAVA-based open source image-processing programme ImageJ (National Institutes of Health, Bethesda, MD).

### Electric Field Exposure and Image Acquisition

Nanosecond, high-voltage electric pulses were generated by a pulse generator that was custom-designed and manufactured at the Laboratory of Biocybernetics at the Faculty of Electrical Engineering, University of Ljubljana, described previously (Rebersek et al. 2009). The pulses were delivered to the electrode chamber: gold electrodes (100  $\mu\text{m}$  apart, 2.1  $\mu\text{m}$  deep) mounted onto a cover glass and placed under the microscope to observe effects in real-time as described earlier (Napotnik et al. 2010). Pulses were measured at each experiment by the calibrated equipment at the electrodes (Batista Napotnik et al. 2016): a LeCroy (Teledyne LeCroy, Chestnut Ridge, NY, USA) PPE2 kV, 400 MHz voltage probe and LeCroy Wave Surfer 422, 200 MHz oscilloscope (Fig. 2—pulse) were used. More than double pulse traveling time through the system (which is 200 ns) was displayed. Hundred pulses of 200 ns and 45 kV/cm were delivered, with repetition rates of 10 Hz or 10 kHz.

**Fig. 2** A typical electric pulse used in our study. Maximal voltage was 450 V and full width at half maximum was 200 ns



Polymersomes were diluted in porating medium (buffers A, AB, B, and C) just before the experiment 1:5 (5  $\mu\text{L}$  of polymersomes and 20  $\mu\text{L}$  of buffer). 25  $\mu\text{L}$  of polymer-some solution was placed between the electrodes and covered with cover glass. Polymersomes were allowed for a few minutes to settle at the bottom of electrode chamber before pulses were delivered.

Images were captured with an epifluorescence microscope (AxioVert 200, Zeiss, Germany, 20 $\times$  objective, with excitation light at 485 nm and appropriate filter set Filter Chroma 41028, Q515 1p BS/HQ535/30 m EM, light exposure time 100 ms) in a time-lapse acquisition mode (30 s, two frames per second). Pulses were delivered at 5 s of image acquisition (manual synchronization). Polymersomes pulsed with the same pulses at high repetition rate (10 kHz) were captured also with faster image acquisition rate: with light exposure time 20 ms and image acquisition each 61 ms for 12.2 s. In this case, pulse application begun at 2 s of image acquisition. In all experiments, the controls were done at exact same conditions only without pulse application.

### Image Analysis

Image analysis was performed by the use of ImageJ software. In analysis, time zero was set at frames immediately before the beginning of pulse application. Deformation of polymersomes was estimated by measuring two orthogonal axes (a) parallel to the electric field and (b) perpendicular to electric field. The semiaxes ratio  $a/b$  was calculated for all polymersomes. The axes were measured with automated particle analysis in ImageJ, in the case of overlapping of polymersomes, measuring was done by hand. Poration was determined in two ways: (1) by the number of visible polymersomes 20 s after the beginning of poration, divided by the number of visible polymersomes immediately before pulse application (at time 0), and (2) by determining an average fluorescence of polymersomes (after/before

poration). This way, we monitored both calcein release and bursting of the vesicles. Visible polymersomes before pulse application (time 0) and 20 s after poration were encircled in fluorescence images, and mean fluorescence of polymersomes was estimated with ImageJ. Throughout the whole study, in three to four separate experiments, all the polymersomes in each image (ranging from 4 to 29) were analyzed. At the beginning of experimenting, mostly 10–20 polymersomes were present in the visible field. The polymersomes that migrated into or out of the field during image acquisition (in 20 s after the poration) were not taken into an account when counting polymersomes. The axes were measured only in polymersomes that were present in the field of vision as whole vesicles.

### Statistical Analysis

Statistical analysis was performed using Excel (Microsoft Corp., Redmond, WA) and SigmaPlot 11.0 (Systat Software, Chicago, IL): the results are expressed as mean  $\pm$  SE, and statistically significant differences ( $p < 0.05$ ) were determined by two- or three- way ANOVA, followed by Bonferroni/Holm–Sidak test, and by Student's test for separate groups.

## Results

### Toxicity of Polymersomes

Polymersomes (SUVs and GUVs) were tested for cytotoxicity on CHO and B16-F1 cells. SUVs with concentrations ranging from 0.025 to 250  $\mu\text{g}/\text{mL}$  were added to cell culture. The mean average diameter of the SUV vesicles was  $68 \pm 7$  nm. After two days of incubation, cytotoxicity was tested with MTS test and it revealed no toxic effects even at the highest of SUVs concentration tested for both cell lines (Fig. 3a).

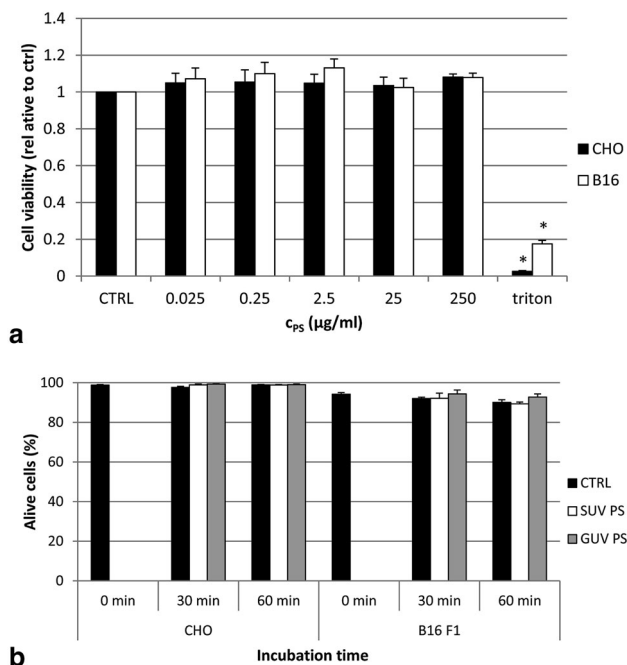


**Fig. 3** **a** MTS 48 h cytotoxicity test of SUV polymerosomes (PS) on CHO (black) and B16-F1 (white) cells. Cell viability is expressed as mean  $\pm$  SE from three independent experiments. 1% Triton X-100 was used as positive control. Significant differences from control are designated by asterisks (\*  $p < 0.05$ ). **b** Short-term cytotoxicity of polymerosomes SUVs (SUV PS, white) and GUVs (GUV PS, gray) on CHO and B16-F1 cells. Buffer B alone served as control (CTRL, black). The percentage of alive cells was determined as propidium iodide-negative. Results are expressed as mean  $\pm$  SE from three independent experiments

Also, polymerosome SUVs and GUVs in highest concentrations tested (1.35 mg/mL for SUVs and stock solution from electroformation of GUVs, unknown concentration) were not cytotoxic in short-term experiments (30 and 60 min after vesicles addition, see Fig. 3b).

### Polymerosome GUV Shape Changes in Electric Field

Polymerosomes with different inner and outer buffers (see Table 1) were exposed to nanosecond electric pulses (100  $\times$  200 ns, 45 kV/cm) of two different repetition rates (10 Hz and 10 kHz). Fluorescence images taken each 0.5 s were analyzed for shape deformations and electroporation (Fig. 4).

Polymerosome GUVs with inner buffer ABc (0.3 M saccharose, 5 mM NaCl, 1 mM calcein, of conductivity 930  $\mu$ S/cm) in poration buffer A (0.3 M glucose, of conductivity 9  $\mu$ S/cm, the  $\lambda_{in}/\lambda_{out}$  conductivity ratio was 103.3) were exposed to a hundred nanosecond electric pulses of 200 ns, 45 kV/cm at repetition rate of 10 Hz or 10 kHz (Fig. 5a, b). At high repetition rate (10 kHz), polymerosomes adopted prolate shape immediately (0.5 s) after pulse application (Fig. 5c), whereas at low repetition

rate (10 Hz), polymerosomes did not significantly differ from control during 12.5 s after the beginning of pulse application (pulse application itself took 10 s). At 10 kHz, the induced prolate shape ( $a/b = 1.37 \pm 0.10$  at 0.5 s after pulse application) was diminished to an almost spherical morphology ( $a/b = 1.08 \pm 0.05$ ) at 1 s after pulse.

In further experiments, we exposed Ac and ABc polymerosome GUVs to the same electric pulses with two repetition rates (10 Hz and 10 kHz) in different poration buffers (A, AB, B, and C; for composition and conductivities see Materials and Methods, Table 1). Vesicles' size ranged from 3 to 19  $\mu$ m in diameter, with the average size of diameter  $9.7 \pm 0.5$   $\mu$ m for Ac and  $8.2 \pm 0.3$   $\mu$ m for ABc polymerosomes. The maximum deformation due to electric pulse exposure was determined. For higher repetition rate (10 kHz), we determined the semiaxes ratio  $a/b$  at 0.5 s after the pulse application and for lower repetition rate (10 Hz) we measured it at 5 s after the beginning of the pulse application. This was based on the results of the deformation of polymerosomes in time (see Fig. 5c). Significant prolate shape deformation was observed with both Ac and ABc polymerosomes but only in buffer A and with higher repetition rate 10 kHz (Fig. 5d). In these cases, the internal conductivities were higher than in the outer media (the  $\lambda_{in}/\lambda_{out}$  conductivity ratios were 53.0 for Ac/A and 103.3 for ABc/A). The two polymerosomes did not differ among themselves, maximum  $a/b$  ratio in buffer A and with 10 kHz pulse train was  $1.41 \pm 0.05$  for Ac and  $1.37 \pm 0.10$  for ABc. In buffer A and repetition rate 10 Hz,  $a/b$  were  $1.08 \pm 0.05$  for Ac and  $1.02 \pm 0.01$  for ABc; however, the ratios were not significantly different from control ( $1.01 \pm 0.01$  and  $1.00 \pm 0.01$  for control Ac and ABc, respectively). In other buffers, the deformation was not detected, i.e.,  $a/b$  was not significantly different from control. In cases where conductivity of the outer buffer was higher than that of the inner buffer, the oblate shape was not observed.

The polymerosomes pulsed with high repetition rate pulse train were also observed with a faster image acquisition rate (one frame each 61 ms, analyzed every 122 ms) to reveal the dynamics of polymerosome deformation at its highest degree (Fig. 6). The prolate deformation occurs immediately after pulse application (already at 122 ms) and is quickly relaxed towards spherical shape. In this case, the ratios  $a/b$  of Ac and ABc were significantly different; however, surprisingly, the Ac polymerosomes were slightly more deformed than ABc despite lower  $\lambda_{in}/\lambda_{out}$  conductivity ratio.

### Polymerosome GUV Permeabilization in Electric Field

We analyzed the effect of electroporation with different pulses and different buffers on electroporation in two ways:

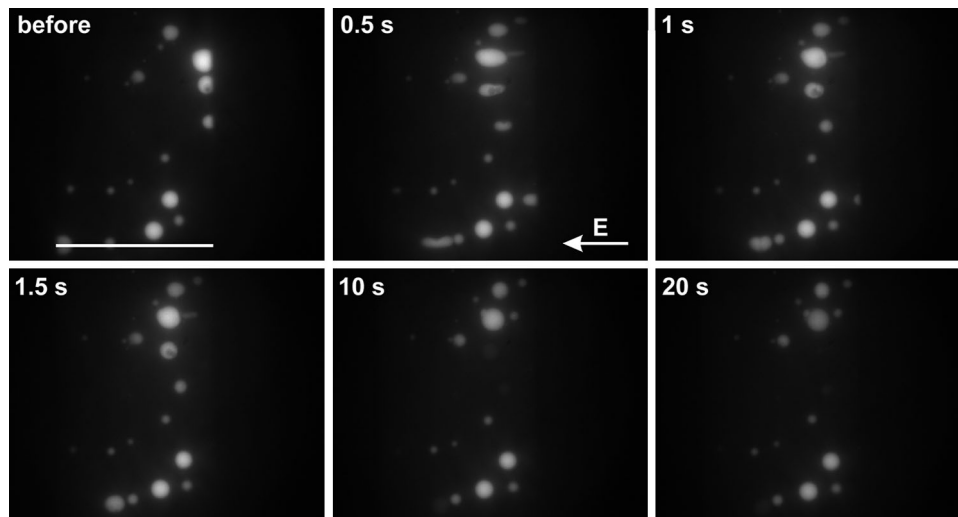


**Fig. 4** The effect of nanosecond electric pulses of high pulse repetition rate (10 kHz): representative sequence of images. The images of Ac polymersomes that were exposed to a hundred pulses of 200 ns, 45 kV/cm, 10 kHz, in buffer A (the  $\lambda_{in}/\lambda_{out}$  conductivity ratio

was 53.0) taken before and after pulse application at times 0.5, 1, 1.5, 10, and 20 s. In the first image (before pulse application), a scale bar shows the position of a 100  $\mu\text{m}$  gap between the electrodes. In the second image (0.5 s), the direction of the electric field is shown

by counting the visible Ac and ABc polymersomes before and 20 s after pulse exposure (Fig. 7), and by measuring the average fluorescence in visible polymersomes (Fig. 8) with the ImageJ software: some vesicles burst or completely lose their calcein (and therefore, the number of vesicles after 20 s is lower than before pulse application) while others, the remaining ones, have lower fluorescence (calcein release).

Polymersomes exposed to nanosecond electric pulses showed significant poration both in total (Fig. 7) and partial (Fig. 8) loss of calcein. The greatest loss of visible polymersomes was with Ac polymersomes in buffer A with 10 kHz pulse repetition rate (on average, the number of visible polymersomes was  $30.0 \pm 7.1\%$  lower than before pulse application); however, the values did not significantly differ between Ac and ABc polymersomes nor the repetition rates. In buffers AB, B, and C (and lower  $\lambda_{in}/\lambda_{out}$  conductivity ratios), the loss of visible polymersomes was not statistically significant for both Ac and ABc polymersomes.

Moreover, different polymersomes (the inner buffers) or repetition rate did not significantly influence average fluorescence in electroporated cells in porating buffer A (Fig. 8). Fluorescence decreased to  $62.0 \pm 2.0$  and  $60.0 \pm 7.2\%$  of initial fluorescence in Ac polymersomes and 10 Hz and 10 kHz, respectively. In ABc, fluorescence decreased to  $71.2 \pm 1.0$  and  $71.4 \pm 4.4\%$  of initial fluorescence for 10 Hz and 10 kHz, respectively. To observe in more details the release of calcein due to poration, we focused on the average inner fluorescence of polymersomes containing Ac and ABc buffers exposed to the outer buffer A (the  $\lambda_{in}/\lambda_{out}$  conductivity ratios were 53.0 for Ac/A and

103.3 for ABc/A), as this gave most likely the greatest effect in terms of deformation and poration. As a result of this observation we conclude that, despite the clear reduction of vesicles' residual fluorescence, there is no statistically significant difference neither with respect to changing the inner buffer nor to changing the pulse repetition rate.

## Discussion

In the past decade, membrane-like structures composed of block copolymers such as polymersomes have appeared to be promising candidates as drug carriers because of their stability and tunable membrane properties (Lee and Feijen 2012; Müller and Landfester 2015). As such, they need to be non-toxic to cells. In previous studies, polymersomes and other polymer structures such as micelles were found to be non-toxic to cells in vitro or exhibit only mild toxicity in the highest concentrations (Li et al. 2007; Katz et al. 2009; Zhang et al. 2012; Qiao et al. 2013; Oliveira et al. 2013; Erfani-Moghadam et al. 2014; Gallon et al. 2015). Our results show that the [PEO]<sub>13</sub>[PBD]<sub>22</sub> polymer in the form of GUVs and SUVs is not toxic to CHO and B16-F1 cell lines up to a concentration of 250  $\mu\text{g}/\text{mL}$  over a period of 48 h or 1.35 mg/mL within the first 60 min of incubation. These results allow us to further explore the polymersomes as drug carriers or for the delivery of membrane proteins to cell membranes in viable cells.

One of the possibilities for drug delivery is electrofusion of polymersomes with cells. While lipid vesicles were already successfully electrofused with cells (Ramos et al.

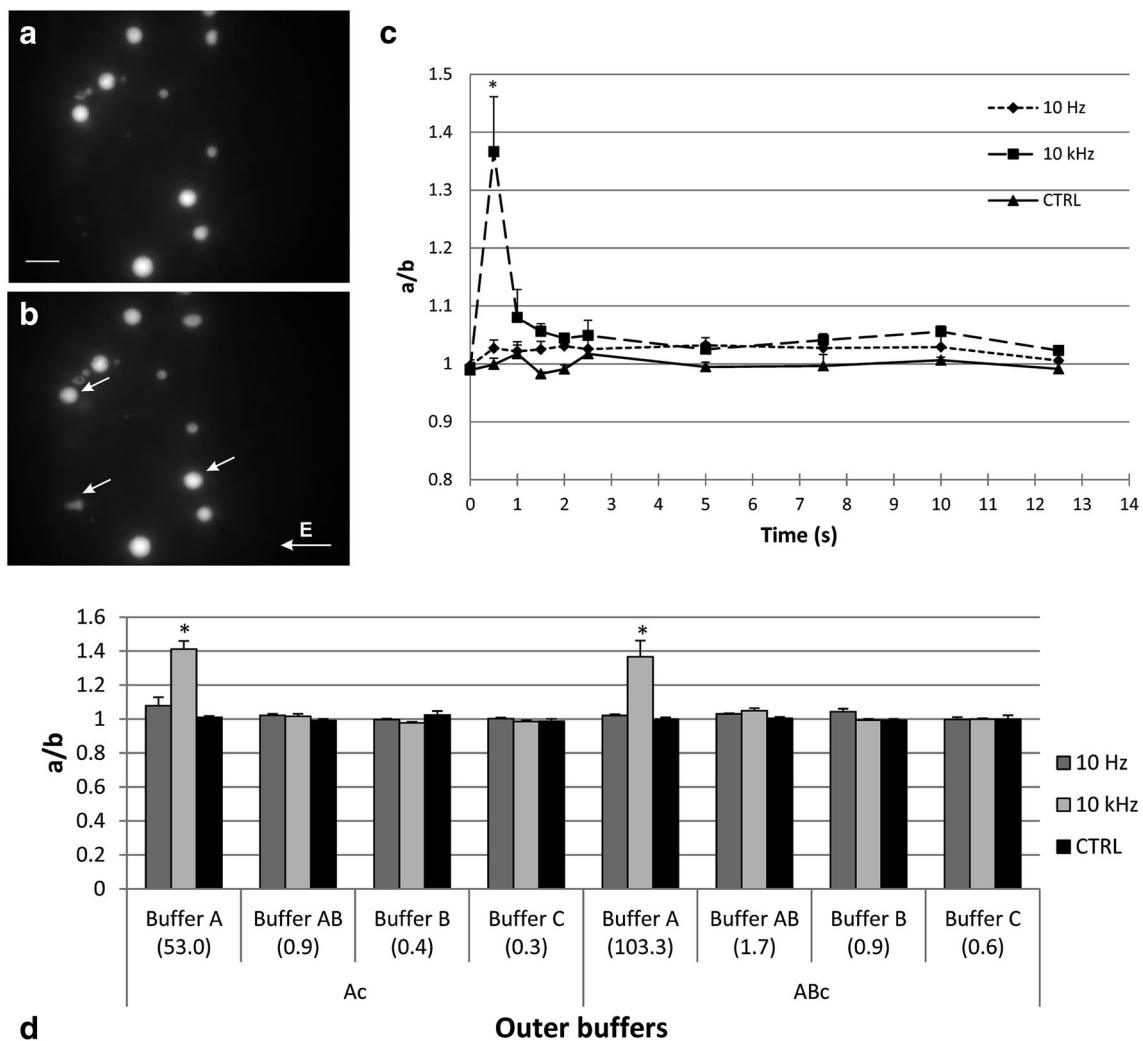


**Fig. 5** The effect of electric pulses on the shape of the polymersome GUVs. **a** Images of ABC polymersome GUVs before pulse application, and **b** 0.5 s after pulse application. GUVs were exposed to a hundred pulses of 200 ns, 45 kV/cm at 10 kHz, in buffer A (the  $\lambda_{in}/\lambda_{out}$  conductivity ratio was 103.3). A scale bar: 20  $\mu$ m. Arrows mark some polymersomes with prolate shape. The direction of the electric field is shown in right lower corner of Fig. 5b. **c** The effect of electric pulses on the shape of ABC polymersome GUVs in time. GUVs were exposed to a hundred pulses of 200 ns, 45 kV/cm at 10 Hz (dotted line) or 10 kHz (dashed line), in buffer A (the  $\lambda_{in}/\lambda_{out}$  conductivity ratio was 103.3). Cells not exposed to pulses served as control (CTRL, full line). The semiaxes ratio  $a/b$  is expressed as mean  $\pm$  SE

from at least three independent experiments. Significant differences from control are designated by asterisks (\*  $p < 0.05$ ). **d** The effect of electric pulses on maximum deformation of polymersome GUVs with inner buffers Ac and ABc in different poration (outer) buffers (with the  $\lambda_{in}/\lambda_{out}$  conductivity ratios in brackets). GUVs were exposed to a hundred pulses of 200 ns, 45 kV/cm at 10 Hz (dark gray) or 10 kHz (light gray), or non-exposed as controls (CTRL, black). For 10 Hz, the maximum deformation was estimated 5 s after the beginning of pulse application and for 10 kHz, it was estimated 0.5 s after pulse exposure. The semiaxes ratio  $a/b$  is expressed as mean  $\pm$  SE from at least three independent experiments. Significant differences from control are designated by asterisks (\*  $p < 0.05$ )

2002; Shirakashi et al. 2012; Lieber et al. 2013; Saito et al. 2014; Raz-Ben Aroush et al. 2015), the electrofusion of polymersomes and cells was not yet achieved. For a successful electrofusion, electroperated membranes as well as close contacts between cells and vesicles are needed (Zimmermann 1982; Usaj et al. 2013). In achieving close contacts by different mechanical methods or by dielectrophoresis (Usaj et al. 2013), the deformation of vesicles due to electric field exposure can play a significant role. In the scope of this study, we investigated electrodeformation

and poration of polymersomes with nanosecond electric pulses. Such short pulses can provoke electrofusion of cells of different sizes (Rems et al. 2013) which is favorable for possible fusion of cells and polymersomes.

In electric field, vesicles are deformed due to the electric stress on the membrane, caused by the Maxwell stress tensor (Riske and Dimova 2005). Our results show that exposing polymersomes to multiple nanosecond pulses can cause deformation of vesicles. The repetition rate as well as the buffer conductivity affects the deformation: the most

**Fig. 6** The deformation of polymersomes pulsed with only high pulse repetition rate (10 kHz), in buffer A (the  $\lambda_{in}/\lambda_{out}$  conductivity ratio was 53.0 for Ac and 103.3 for ABc) recorded with a faster image acquisition rate (*a/b* is analyzed every 122 ms). GUVs were exposed to a hundred pulses of 200 ns, 45 kV/cm at 10 kHz. The semiaxes ratio *a/b* is expressed as mean  $\pm$  SE from six independent experiments

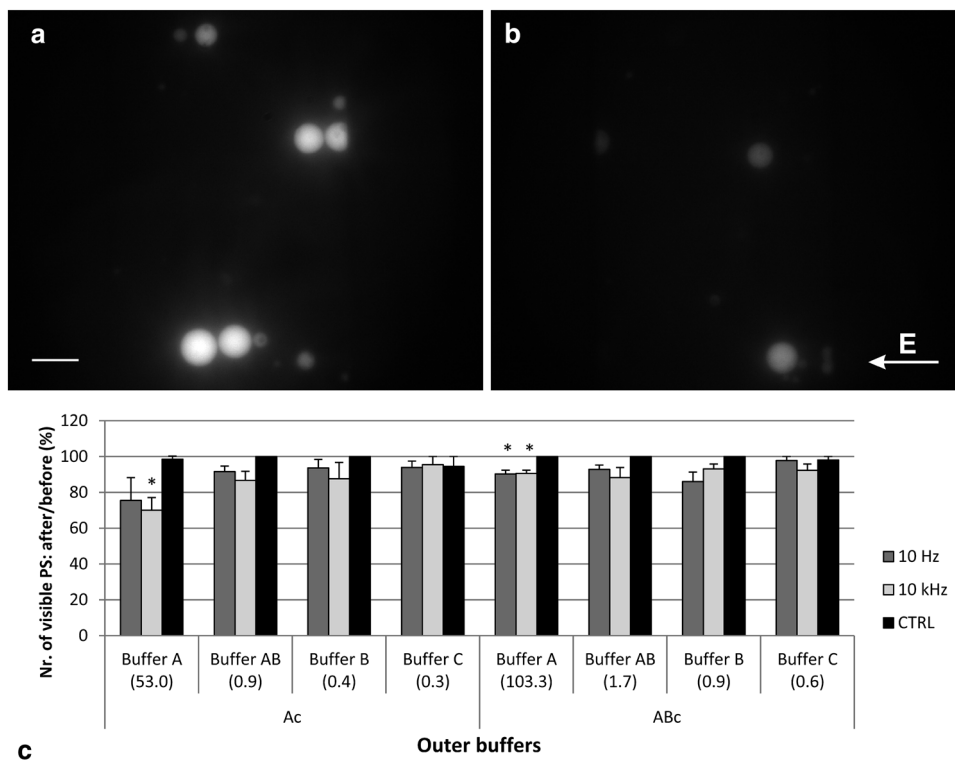
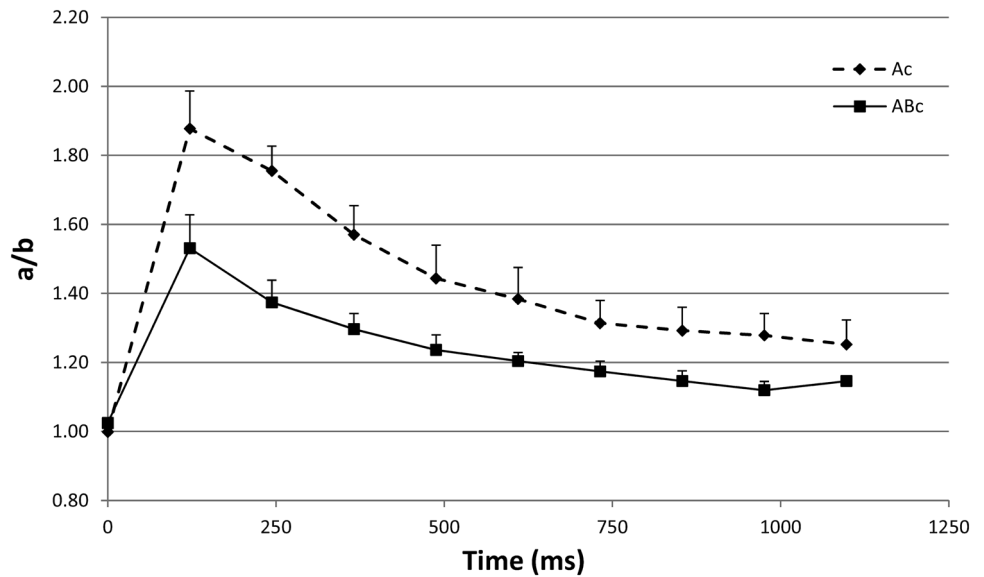


**Fig. 7** The effect of electric pulses on the poration of Ac polymer-some GUVs. **a** Images before pulse application, and **b** 20 s after pulse application. GUVs were exposed to a hundred pulses of 200 ns, 45 kV/cm at 10 kHz, in buffer A (the  $\lambda_{in}/\lambda_{out}$  conductivity ratio was 53.0). A scale bar: 20  $\mu$ m. The direction of the electric field is shown in right lower corner of **(b)**. **c** The effect of electric pulses on the poration of polymersome GUVs with inner buffers Ac and ABc in different poration (outer) buffers (with the  $\lambda_{in}/\lambda_{out}$  conductivity ratios

in brackets). GUVs were exposed to a hundred pulses of 200 ns, 45 kV/cm at 10 Hz (dark gray) or 10 kHz (light gray), or non-exposed as controls (CTRL, black). The ratio of visible polymersomes (PS) 20 s after the beginning of pulse application and before pulse application (in percentages) is expressed as mean  $\pm$  SE from at least three independent experiments. Significant differences from control are designated by asterisks (\*  $p < 0.05$ )

pronounced deformation into prolate form (along the axis of the electric field) was seen in buffer with the lowest conductivity (buffer A, 9  $\mu$ S/cm) and high repetition rate

(10 kHz). For AC fields, it is already known that the electric field frequency and buffer conductivities affect the deformation of lipid or polymer vesicles (Dimova et al.

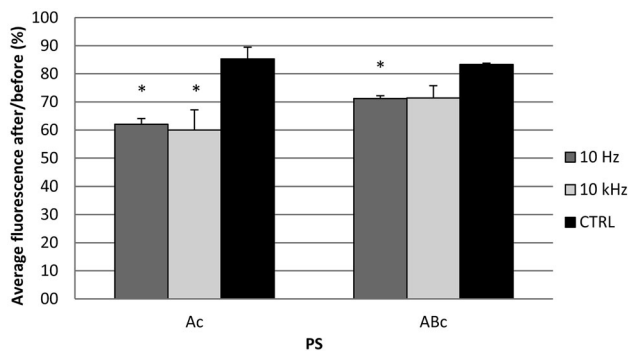


**Fig. 8** The effect of electric pulses on the average fluorescence of GUV polymersomes (PS) with inner buffers Ac and ABc in poration (outer) buffer A (the  $\lambda_{in}/\lambda_{out}$  conductivity ratios were 53.0 and 103.3, respectively). GUVs were exposed to a hundred pulses of 200 ns, 45 kV/cm at 10 Hz (dark gray) or 10 kHz (light gray), or non-exposed as controls (CTRL, black). The ratio of average fluorescence 20 s after the beginning of pulse application and before pulse application (in percentages) is expressed as mean  $\pm$  SE from at least three independent experiments. Significant differences from control are designated by asterisks (\*  $p < 0.05$ )

2007; Aranda et al. 2008; Yamamoto et al. 2010; Salipante et al. 2012). In DC fields, the same deformations are expected according to the inverse of the pulse duration (Neumann et al. 1998; Dimova et al. 2007; Sadik et al. 2011; Salipante and Vlahovska 2014); however, the effect of multiple DC pulses on vesicle shape changes was not yet thoroughly explored. Monitoring deformation of polymersomes in low conductivity buffer revealed that, in contrast to high repetition rate, low repetition rate (10 Hz) pulses did not cause detectable deformation the whole time of pulse application and a few seconds later. With higher repetition rate, pulses seem to have an additive effect which is more likely to build up a greater Maxwell stress and induce deformation, in this case of prolate shape. Whereas with low repetition rate, pulses act separate from each other and the stress induced on the membrane is lower.

The development of a prolate shape in conductivity buffer conditions of  $\lambda_{in} > \lambda_{out}$  is a consequence of the inner pressure exerted by the movement of ions within the vesicle along the EF direction. Inversely, when  $\lambda_{in} < \lambda_{out}$ , ions from the outside compress the vesicle to an oblate shape (perpendicular to the electric field) (Dimova et al. 2007; Aranda et al. 2008; Yamamoto et al. 2010; Salipante and Vlahovska 2014). In our studies, the appearance of a prolate shape diminished with increasing outer conductivity. However, in cases where  $\lambda_{in} < \lambda_{out}$ , we did not detect any oblate shape and the polymersomes did not significantly differ from control vesicles which retained spherical shape. This could be possibly due to a too low difference in conductivities between inner and outer buffers. Such effect was observed for all polymersomes irrespective of their

inner conductivities (Ac: 477  $\mu$ S/cm, ABc: 930  $\mu$ S/cm). Fast recording revealed that, surprisingly, Ac polymersomes were slightly more deformed than ABc despite the latter has a higher conductivity and ions content than the former. The reason of such behavior is not known and further experiment aim to address it.

The occurrence of prolate-shaped polymersomes in low conductivity buffer can be advantageous for possible fusion of vesicles or cells and polymersomes (Liu et al. 2016): (1) prolate vesicles in low conductivity outer buffers can be selectively electroporated at the contact area between two vesicles, according to simulations of Liu (Liu et al. 2016); (2) a low buffer conductivity is required for cell alignment into a pearl-chain with dielectrophoresis, which is one of the methods for achieving cell/vesicle contact (Rems et al. 2013; Liu et al. 2016); (3) simulations and experiments showed that fusion is more efficient in hypotonic medium due to a mild swelling of the vesicles (Usaj and Kanduser 2012; Rems et al. 2013); and (4) finally, the prolate shape of vesicles pulsed while they are in a pearl-chain may increase the contact area of vesicles, or cells, encouraging the fusion process.

Most studies on GUV deformation in electric fields were performed with fast cameras due to the short state of the deformation and fast relaxation to initial spherical shape after pulse ending (Riske and Dimova 2005, 2006; Dimova et al. 2007). In our study, the vesicle deformation was seen even with slow recording (two frames per s) and the relaxation lasted a few seconds after the pulse train application. Compared to lipid vesicles, polymersomes have a thicker membrane and higher viscosity, leading to a slower response and relaxation (Riske and Dimova 2005; Salipante and Vlahovska 2014). Moreover, it was observed earlier that porated lipid vesicles took a longer time (up to 20 s) to relax compared to non-porated ones (Riske and Dimova 2005; Riske et al. 2009).

Besides deformation, we also observed electroporation of polymersomes with multiple nanosecond electric pulses. This was detected by a decrease in number of visible polymersomes after pulse application and by the loss of calcein from the vesicles. Poration was most pronounced in low conductivity outer buffer which is in agreement with previous reports for lipid vesicles (Teissie and Tsong 1981; Neumann and Kakorin 2000; Tekle et al. 2005). Generally, the pore opening lasted considerably long, in fact, the fluorescence kept decreasing even more than 10 s after pulse application. In previous reports, the electropores in lipid vesicles took much shorter time (tens to a few hundred milliseconds) to reseal (Tekle et al. 2001; Riske and Dimova 2005); however, the extent of electroporation depends on pulse parameters, namely electric field strength and pulse number (Teissie and Tsong 1981; Tekle et al. 2005; Mauroy et al. 2012; Salipante and Vlahovska 2014).

It was already shown that the pore lifetime in polymersomes is much longer than in lipid vesicles (Aranda-Espinoza et al. 2001; Bermúdez et al. 2003; Riske and Dimova 2005; Photos et al. 2007) which is also due to polymersome stability and higher viscosity (Dimova et al. 2002; Riske and Dimova 2005). In polymersomes composed of much longer polymer chains than the ones used in our study (PEO<sub>80</sub>-PBD<sub>125</sub> or larger, and PEO<sub>13</sub>-PBD<sub>22</sub>, respectively), large, stable pores can be sterically stabilized by PEG chains in the inner structure (Photos et al. 2007).

Interestingly, our results show that the electroporation extent in polymersomes was similar at both high (10 kHz) and low (10 Hz) pulse repetition rates, despite the fact that higher repetition rate led to higher deformation into the prolate ellipsoid shape (in low conductivity buffer). This effect was, to some extent, surprising and it is in contrast with previous models and experimental results performed on lipid membranes. In lipid membranes, the critical voltage for membrane breakdown is lower with higher membrane tension (Needham and Hochmuth 1989; Zhelev and Needham 1993; Riske and Dimova 2005; Dimova et al. 2007). Consequently, it is expected that in our case, higher repetition rate would lead to more electroporation, however, it did not. The electrodeformation (the ratio *ab* of around 1.4) may be too small to have an effect on such tough vesicles with a high lysis tension (Discher et al. 1999; Dimova et al. 2002). This is in agreement with a report where even with higher deformation of polymersomes in higher electric field, the frequency of the applied AC field required for the prolate to oblate transition did not change, indicating that membranes did not undergo significant thinning in the voltage range investigated (Salipante et al. 2012).

## Conclusion

In conclusion, polymersomes used in our study (PEO<sub>13</sub>-PBD<sub>22</sub>) did not reveal any toxic activity in vitro for the two cell lines tested and are therefore suitable for further investigation for possible electrofusion with cells. By exposing polymersomes to nanosecond electric pulses (100 × 200 ns, 45 kV/cm) we achieved their electroporation; however, the electrodeformation in the direction of electric field (prolate shape) can only be seen with high pulse repetition rate (10 kHz) at conductivity conditions of  $\lambda_{in} > \lambda_{out}$ . Oblate shape at conductivity conditions of  $\lambda_{in} < \lambda_{out}$  was not observed. This can be advantageous for possible cell-polymersome electrofusion. Within this work, we explored the putative use of polymersomes as carrier systems for membrane-associated or even integral membrane proteins. In plane fusion of polymeric membrane alternative materials, e.g., the polymersomes, with lipidic

liposomes and ultimately with cells, can pave the way for novel strategies in membrane protein delivery. With this work, we have investigated some of the prerequisite conditions in generating such hybrid membrane architectures by nanosecond pulse electrofusion.

**Acknowledgement** The study was supported by the Austrian Science Fund (FWF) and Slovenian Research Agency (ARRS)—Austrian-Slovenian Lead Agency Joint Project: Electroporation as Method for Inserting Functional Membrane Proteins in Mammalian Cells N2-0027 (2015-2017), and by Austrian-Slovenian Lead Agency Joint Project: Electroporation as Method for Inserting Functional Membrane Proteins in Mammalian Cells BI-AT/16-17-003 (2015-2017). It was conducted in the scope of the LEA EBAM: European Laboratory of Pulsed Electric Fields Applications in Biology and Medicine (2011-2018).

## References

- Ahmed F, Discher DE (2004) Self-porating polymersomes of PEG-PLA and PEG-PCL: hydrolysis-triggered controlled release vesicles. *J Control Release Off J Control Release Soc* 96:37–53. doi:10.1016/j.jconrel.2003.12.021
- Alberts B, Johnson A, Lewis J et al (2002) Ion channels and the electrical properties of membranes. In: *Molecular biology of the cell*, 4th edn. Garland Science, New York. Available from <https://www.ncbi.nlm.nih.gov/books/NBK26910/>
- Angelova MI, Dimitrov DS (1986) Liposome electroformation. *Faraday Discuss Chem Soc* 81:303–311. doi:10.1039/DC9868100303
- Aranda S, Riske KA, Lipowsky R, Dimova R (2008) Morphological transitions of vesicles induced by alternating electric fields. *Biophys J* 95:L19–21. doi:10.1529/biophysj.108.132548
- Aranda-Espinoza H, Bermudez H, Bates FS, Discher DE (2001) Electromechanical limits of polymersomes. *Phys Rev Lett* 87:208301. doi:10.1103/PhysRevLett.87.208301
- Bain J, Ruiz-Pérez L, Kennerley AJ et al (2015) In situ formation of magnetopolymersomes via electroporation for MRI. *Sci Rep* 5:14311. doi:10.1038/srep14311
- Bartrop JA, Owen TC, Cory AH, Cory JG (1991) 5-(3-carboxymethoxyphenyl)-2-(4,5-dimethylthiazolyl)-3-(4-sulfophenyl)tetrazolium, inner salt (MTS) and related analogs of 3-(4,5-dimethylthiazolyl)-2,5-diphenyltetrazolium bromide (MTT) reducing to purple water-soluble formazans As cell-viability indicators. *Bioorg Med Chem Lett* 1:611–614. doi:10.1016/S0960-894X(01)81162-8
- Batista Napotnik T, Reberšek M, Vernier PT et al (2016) Effects of high voltage nanosecond electric pulses on eukaryotic cells (in vitro): a systematic review. *Bioelectrochem Amst Neth* 110:1–12. doi:10.1016/j.bioelechem.2016.02.011
- Bermudez H, Brannan AK, Hammer DA et al (2002) Molecular weight dependence of polymersome membrane structure, elasticity, and stability. *Macromolecules* 35:8203–8208. doi:10.1021/ma020669i
- Bermúdez H, Aranda-Espinoza H, Hammer DA, Discher DE (2003) Pore stability and dynamics in polymer membranes. *EPL Europhys Lett* 64:550. doi:10.1209/epl/i2003-00264-2
- Dimova R, Seifert U, Pouligny B et al (2002) Hyperviscous diblock copolymer vesicles. *Eur Phys J E* 7:241–250. doi:10.1140/epje/i200101032
- Dimova R, Riske KA, Aranda S et al (2007) Giant vesicles in electric fields. *Soft Matter* 3:817–827. doi:10.1039/B703580B

- Dimova R, Bezlyepkina N, Jordö MD et al (2009) Vesicles in electric fields: some novel aspects of membrane behavior. *Soft Matter* 5:3201–3212. doi:[10.1039/B901963D](https://doi.org/10.1039/B901963D)
- Discher BM, Won YY, Ege DS et al (1999) Polymersomes: tough vesicles made from diblock copolymers. *Science* 284:1143–1146
- Discher BM, Bermudez H, Hammer DA et al (2002) Cross-linked polymersome membranes: vesicles with broadly adjustable properties. *J Phys Chem B* 106:2848–2854. doi:[10.1021/jp011958z](https://doi.org/10.1021/jp011958z)
- Erfani-Moghadam V, Nomani A, Zamani M et al (2014) A novel diblock of copolymer of (monomethoxy poly [ethylene glycol]-oleate) with a small hydrophobic fraction to make stable micelles/polymersomes for curcumin delivery to cancer cells. *Int J Nanomed* 9:5541–5554. doi:[10.2147/IJN.S63762](https://doi.org/10.2147/IJN.S63762)
- Gabriel B, Teissié J (1995) Control by electrical parameters of short- and long-term cell death resulting from electroporation of Chinese hamster ovary cells. *Biochim Biophys Acta* 1266:171–178
- Gallon E, Matini T, Sasso L et al (2015) Triblock copolymer nanovesicles for pH-responsive targeted delivery and controlled release of siRNA to cancer cells. *Biomacromol* 16:1924–1937. doi:[10.1021/acs.biomac.5b00286](https://doi.org/10.1021/acs.biomac.5b00286)
- Israelachvili JN (2011) *Intermolecular and surface forces*, 3rd edn. Academic Press, Santa Barbara
- Jordan CA, Neumann E, Sowers AE (2013) *Electroporation and electrofusion in cell biology*. Springer Science & Business Media, New York
- Katz JS, Levine DH, Davis KP et al (2009) Membrane stabilization of biodegradable polymersomes. *Langmuir ACS J Surf Colloids* 25:4429–4434. doi:[10.1021/la803769q](https://doi.org/10.1021/la803769q)
- Knorr RL, Staykova M, Gracià RS, Dimova R (2010) Wrinkling and electroporation of giant vesicles in the gel phase. *Soft Matter* 6:1990–1996. doi:[10.1039/B925929E](https://doi.org/10.1039/B925929E)
- Kotnik T, Miklavcic D (2000) Second-order model of membrane electric field induced by alternating external electric fields. *IEEE Trans Biomed Eng* 47:1074–1081. doi:[10.1109/10.855935](https://doi.org/10.1109/10.855935)
- Kotnik T, Miklavcic D, Slivnik T (1998) Time course of transmembrane voltage induced by time-varying electric fields—a method for theoretical analysis and its application. *Bioelectrochem Bioenerg* 45:3–16. doi:[10.1016/S0302-4598\(97\)00093-7](https://doi.org/10.1016/S0302-4598(97)00093-7)
- Le Meins J-F, Sandre O, Lecommandoux S (2011) Recent trends in the tuning of polymersomes' membrane properties. *Eur Phys J E Soft Matter* 34:14. doi:[10.1140/epje/i2011-11014-y](https://doi.org/10.1140/epje/i2011-11014-y)
- Lee JS, Feijen J (2012) Polymersomes for drug delivery: design, formation and characterization. *J Control Release Off J Control Release Soc* 161:473–483. doi:[10.1016/j.jconrel.2011.10.005](https://doi.org/10.1016/j.jconrel.2011.10.005)
- Li S, Byrne B, Welsh J, Palmer AF (2007) Self-assembled poly(butadiene)-b-poly(ethylene oxide) polymersomes as paclitaxel carriers. *Biotechnol Prog* 23:278–285. doi:[10.1021/bp060208+](https://doi.org/10.1021/bp060208+)
- Lieber AD, Yehudai-Resheff S, Barnhart EL et al (2013) Membrane tension in rapidly moving cells is determined by cytoskeletal forces. *Curr Biol CB* 23:1409–1417. doi:[10.1016/j.cub.2013.05.063](https://doi.org/10.1016/j.cub.2013.05.063)
- Liu L, Mao Z, Zhang J et al (2016) The influence of vesicle shape and medium conductivity on possible electrofusion under a pulsed electric field. *PLoS ONE* 11:e0158739. doi:[10.1371/journal.pone.0158739](https://doi.org/10.1371/journal.pone.0158739)
- Lodish H, Berk A, Zipursky SL et al (2000) *Molecular cell biology*, 4th edn. W. H. Freeman, New York
- Mauroy C, Portet T, Winterhalder M et al (2012) Giant lipid vesicles under electric field pulses assessed by non invasive imaging. *Bioelectrochem Amst Neth* 87:253–259. doi:[10.1016/j.bioelechem.2012.03.008](https://doi.org/10.1016/j.bioelechem.2012.03.008)
- Mayer LD, Hope MJ, Cullis PR (1986) Vesicles of variable sizes produced by a rapid extrusion procedure. *Biochim Biophys Acta* 858:161–168
- Müller LK, Landfester K (2015) Natural liposomes and synthetic polymeric structures for biomedical applications. *Biochem Biophys Res Commun* 468:411–418. doi:[10.1016/j.bbrc.2015.08.088](https://doi.org/10.1016/j.bbrc.2015.08.088)
- Napotnik TB, Reberšek M, Kotnik T et al (2010) Electroporation of endocytotic vesicles in B16 F1 mouse melanoma cells. *Med Biol Eng Comput* 48:407–413. doi:[10.1007/s11517-010-0599-9](https://doi.org/10.1007/s11517-010-0599-9)
- Needham D, Hochmuth RM (1989) Electro-mechanical permeabilization of lipid vesicles. Role of membrane tension and compressibility. *Biophys J* 55:1001–1009
- Neumann E, Kakorin S (2000) Electroporation of curved lipid membranes in ionic strength gradients. *Biophys Chem* 85:249–271
- Neumann E, Kakorin S, Toensing K (1998) Membrane electroporation and electromechanical deformation of vesicles and cells. *Faraday Discuss* 111:125–157
- Oliveira H, Pérez-Andrés E, Thevenot J et al (2013) Magnetic field triggered drug release from polymersomes for cancer therapeutics. *J Control Release Off J Control Release Soc* 169:165–170. doi:[10.1016/j.jconrel.2013.01.013](https://doi.org/10.1016/j.jconrel.2013.01.013)
- Perrier DL, Rems L, Boukany PE (2017) Lipid vesicles in pulsed electric fields: fundamental principles of the membrane response and its biomedical applications. *Adv Colloid Interface Sci*. doi:[10.1016/j.cis.2017.04.016](https://doi.org/10.1016/j.cis.2017.04.016)
- Photos PJ, Bermudez H, Aranda-Espinoza H et al (2007) Nuclear pores and membrane holes: generic models for confined chains and entropic barriers in pore stabilization. *Soft Matter* 3:364–371. doi:[10.1039/B611412C](https://doi.org/10.1039/B611412C)
- Qiao Z-Y, Ji R, Huang X-N et al (2013) Polymersomes from dual responsive block copolymers: drug encapsulation by heating and acid-triggered release. *Biomacromol* 14:1555–1563. doi:[10.1021/bm400180n](https://doi.org/10.1021/bm400180n)
- Ramos C, Bonato D, Winterhalter M et al (2002) Spontaneous lipid vesicle fusion with electroporated cells. *FEBS Lett* 518:135–138
- Raz-Ben Aroush D, Yehudai-Resheff S, Keren K (2015) Electrofusion of giant unilamellar vesicles to cells. *Methods Cell Biol* 125:409–422. doi:[10.1016/bs.mcb.2014.11.005](https://doi.org/10.1016/bs.mcb.2014.11.005)
- Reberšek M, Kranjc M, Pavliha D et al (2009) Blumlein configuration for high-repetition-rate pulse generation of variable duration and polarity using synchronized switch control. *IEEE Trans Biomed Eng* 56:2642–2648. doi:[10.1109/TBME.2009.2027422](https://doi.org/10.1109/TBME.2009.2027422)
- Rems L, Usaj M, Kanduser M et al (2013) Cell electrofusion using nanosecond electric pulses. *Sci Rep* 3:3382. doi:[10.1038/srep03382](https://doi.org/10.1038/srep03382)
- Riske KA, Dimova R (2005) Electro-deformation and poration of giant vesicles viewed with high temporal resolution. *Biophys J* 88:1143–1155. doi:[10.1529/biophysj.104.050310](https://doi.org/10.1529/biophysj.104.050310)
- Riske KA, Dimova R (2006) Electric pulses induce cylindrical deformations on giant vesicles in salt solutions. *Biophys J* 91:1778–1786. doi:[10.1529/biophysj.106.081620](https://doi.org/10.1529/biophysj.106.081620)
- Riske KA, Knorr RL, Dimova R (2009) Bursting of charged multicomponent vesicles subjected to electric pulses. *Soft Matter* 5:1983–1986. doi:[10.1039/B900548J](https://doi.org/10.1039/B900548J)
- Sadik MM, Li J, Shan JW et al (2011) Vesicle deformation and poration under strong DC electric fields. *Phys Rev E* 83:66316. doi:[10.1103/PhysRevE.83.066316](https://doi.org/10.1103/PhysRevE.83.066316)
- Saito AC, Ogura T, Fujiwara K et al (2014) Introducing micrometer-sized artificial objects into live cells: a method for cell-giant unilamellar vesicle electrofusion. *PLoS ONE* 9:e106853. doi:[10.1371/journal.pone.0106853](https://doi.org/10.1371/journal.pone.0106853)
- Salipante PF, Vlahovska PM (2014) Vesicle deformation in DC electric pulses. *Soft Matter* 10:3386–3393. doi:[10.1039/C3SM52870G](https://doi.org/10.1039/C3SM52870G)
- Salipante PF, Knorr RL, Dimova R, Vlahovska PM (2012) Electrodeformation method for measuring the capacitance of bilayer membranes. *Soft Matter* 8:3810–3816. doi:[10.1039/C2SM07105C](https://doi.org/10.1039/C2SM07105C)

- Shirakashi R, Sukhorukov VL, Reuss R et al (2012) Effects of a pulse electric field on electrofusion of giant unilamellar vesicle (GUV)-Jurkat cell. *J Therm Sci Technol* 7:589–602. doi:[10.1299/jtst.7.589](https://doi.org/10.1299/jtst.7.589)
- Singer SJ, Nicolson GL (1972) The fluid mosaic model of the structure of cell membranes. *Science* 175:720–731. doi:[10.1126/science.175.4023.720](https://doi.org/10.1126/science.175.4023.720)
- Taubert A, Napoli A, Meier W (2004) Self-assembly of reactive amphiphilic block copolymers as mimetics for biological membranes. *Curr Opin Chem Biol* 8:598–603. doi:[10.1016/j.cbpa.2004.09.008](https://doi.org/10.1016/j.cbpa.2004.09.008)
- Teissie J, Tsong TY (1981) Electric field induced transient pores in phospholipid bilayer vesicles. *Biochemistry (Mosc)* 20:1548–1554
- Tekle E, Astumian RD, Friauf WA, Chock PB (2001) Asymmetric pore distribution and loss of membrane lipid in electroporated DOPC vesicles. *Biophys J* 81:960–968. doi:[10.1016/S0006-3495\(01\)75754-2](https://doi.org/10.1016/S0006-3495(01)75754-2)
- Tekle E, Oubrahim H, Dzekunov SM et al (2005) Selective field effects on intracellular vacuoles and vesicle membranes with nanosecond electric pulses. *Biophys J* 89:274–284. doi:[10.1529/biophysj.104.054494](https://doi.org/10.1529/biophysj.104.054494)
- Usaj M, Kanduser M (2012) The systematic study of the electroporation and electrofusion of B16-F1 and CHO cells in isotonic and hypotonic buffer. *J Membr Biol* 245:583–590. doi:[10.1007/s00232-012-9470-2](https://doi.org/10.1007/s00232-012-9470-2)
- Usaj M, Flisar K, Miklavcic D, Kanduser M (2013) Electrofusion of B16-F1 and CHO cells: the comparison of the pulse first and contact first protocols. *Bioelectrochem Amst Neth* 89:34–41. doi:[10.1016/j.bioelechem.2012.09.001](https://doi.org/10.1016/j.bioelechem.2012.09.001)
- Wang L, Chierico L, Little D et al (2012) Encapsulation of biomacromolecules within polymersomes by electroporation. *Angew Chem Int Ed* 51:11122–11125. doi:[10.1002/anie.201204169](https://doi.org/10.1002/anie.201204169)
- Yamamoto T, Aranda-Espinoza S, Dimova R, Lipowsky R (2010) Stability of spherical vesicles in electric fields. *Langmuir ACS J Surf Colloids* 26:12390–12407. doi:[10.1021/la1011132](https://doi.org/10.1021/la1011132)
- Zhang J, Wu L, Meng F et al (2012) pH and reduction dual-bioresponsive polymersomes for efficient intracellular protein delivery. *Langmuir ACS J Surf Colloids* 28:2056–2065. doi:[10.1021/la203843m](https://doi.org/10.1021/la203843m)
- Zhelev DV, Needham D (1993) Tension-stabilized pores in giant vesicles: determination of pore size and pore line tension. *Biochim Biophys Acta* 1147:89–104
- Zimmermann U (1982) Electric field-mediated fusion and related electrical phenomena. *Biochim Biophys Acta* 694:227–277